Stress–optical behaviour near the T_g and melt flow-induced anisotropy in amorphous polymers

R. Muller* and J. J. Pesce
Ecole d'Application des Hauts Polymères, 4 rue Boussingault, 67000 Strasbourg, France
(Received 27 November 1992; revised 8 July 1993)

Tensile stress and birefringence in polystyrene and polycarbonate melts have been measured at various temperatures during constant strain rate elongational flow. Deviations from the linear stress–optical rule appear at temperatures close to the T_g and are discussed by considering the total stress as the sum of an entropic and a non-entropic contribution. Anisotropy of properties below the T_g of samples where the chain orientation has been frozen-in by quenching, was characterized by thermal expansion measurements. A significant elastic recovery is found to occur at temperatures as low as T_g–30°C, and is discussed as a function of the thermomechanical history.

(Keywords: stress–optical law; birefringence; polymer melt)

INTRODUCTION

In polymer melts undergoing flow, the chains become oriented as a consequence of the applied stress field, with this molecular orientation giving rise, in turn, to birefringence. On the other hand, many properties of polymers in the glassy state (such as Young's modulus, the thermal expansion coefficient or the thermal conductivity) become anisotropic in samples where the chains are oriented[1]. This is typically the case in injection moulded parts in which the polymeric material undergoes high stress levels during flow in the molten state and where quenching below T_g occurs before complete relaxation of the chain orientation.

For melt temperatures well above the T_g, it is usually verified that the stress and polarizability tensors are proportional to each other[2], which is obvious if one assumes Gaussian chain statistics. If this is the case, the anisotropy of properties in the glassy state for samples deformed in the melt and quenched below the T_g can unambiguously be studied as a function of the frozen-in birefringence. This approach has proven successful in describing experimental data on modulus and thermal expansion anisotropy obtained for various amorphous polymers such as polycarbonate (PC) and polystyrene (PS)[1,3].

However if the melt temperature becomes close to the T_g, significant deviations from the linear stress–optical rule have been reported[4–6], and the question arises as to whether the birefringence is in fact the only parameter which controls the anisotropy of glassy state properties.

It is the aim of this present paper to study in more detail the stress–optical behaviour of amorphous polymers at temperatures close to the T_g and to investigate the dependence of anisotropy in the glassy state on the frozen-in birefringence, for the case where the linear stress–optical rule is no longer verified. The experimental method we adopted consists in (a) stretching specimens above the T_g, (b) freezing the orientation by quenching the stretched samples under well-defined conditions, and (c) characterizing the anisotropy in the glassy state by measuring the thermal expansion below the T_g.

EXPERIMENTAL

Two commercially available polymers have been used in this present study, namely polystyrene, obtained from Elf Atochem (®Lacqrene 1241H) and polycarbonate (PC) which was obtained from Bayer (®Makrolon 2805). The glass transition temperatures of these two polymers, as determined by d.s.c., are 95 and 145°C for PS and PC, respectively.

The stress–optical behaviour was characterized in uniaxial extension by using a previously described apparatus that had been designed at our laboratory[7]. Parallelepipedic-shaped specimens can be stretched either at constant elongational strain rate over the range 10^{-4}–1 s^{-1}, or at a constant true tensile stress σ up to values of the extension ratio λ ($=L/L_0$) of approximately 20. For the tests at constant stress, the cross sectional area is calculated by assuming constant volume. During the experiment, the specimen remains in a silicone oil bath which gives a temperature control with a precision of ± 0.1°C over the range between room temperature and 200°C. At the same time, buoyancy prevents low-viscosity samples from flowing under their own weight. The stretched sample can be quickly removed from the oil bath which allows fast quenching to be achieved. The actual cooling rate is limited by the sample thickness: for typical values of the final thickness of approximately 0.3 mm, it takes less than 5 s for the temperature to decrease from 120 to below 80°C within the whole sample. The birefringence is measured during the test by the technique described in ref. 7. Symmetric displacement of

* To whom correspondence should be addressed

0032-3861/94/04/0734–06

the clamps allows the measurements to be carried out near to the central part of the specimen, where the deformation is not affected by any end-effects due to clamping.

The modulus and thermal expansion coefficient in the direction of stretching has been measured for oriented and quenched PS specimens with a Rheometrics RSA-II mechanical spectrometer. For the thermal expansion measurements, the apparatus is driven at zero tensile force and the sample length is recorded as a function of temperature. As reported in the literature[1], we found that Young's modulus in the direction of stretching was little affected by the frozen-in chain orientation. In the following we will therefore mainly consider thermal expansion data for characterizing the anisotropy in the glassy state.

RESULTS AND DISCUSSION

Stress–optical law above the T_g

For temperatures typically above $T_g + 20°C$, a one-to-one relationship between the true stress σ and the birefringence Δn is found for both polymers. In this temperature range, the stress–optical law is independent of both temperature and strain rate[7,8]. As shown in *Figure 1*, the birefringence *versus* stress curves are linear at low stresses: $\sigma \leqslant 2$ MPa for PS and $\sigma \leqslant 4$ MPa for PC. A stress–optical coefficient C_r in the rubbery or molten state can be determined as the initial slope of these curves: for polystyrene, we find that $C_r \approx 4.8 \times 10^{-9}$ Pa^{-1} and for polycarbonate, $C_r \approx 5.9 \times 10^{-9}$ Pa^{-1}, in good agreement with the literature data[4,9]. Our results confirm that C_r is positive for PC and negative for PS, due to the fact that the polarizability of the backbone of the PS chain is lowest in the chain direction. In *Figure 1* and in the following, we have actually taken the absolute value of the birefringence. The deviation from the linear stress–optical rule which is observed at high stresses can be qualitatively explained by a finite chain extensibility which results in a saturation of the orientation[10]. It is important to note that if the temperature is high enough, the relationship between σ and Δn is independent of temperature and strain rate, even in its non-linear part. The curves in *Figure 1*, which are characteristic of the behaviour of the melt at temperatures which are high enough with respect to the T_g, will therefore be called 'equilibrium' curves.

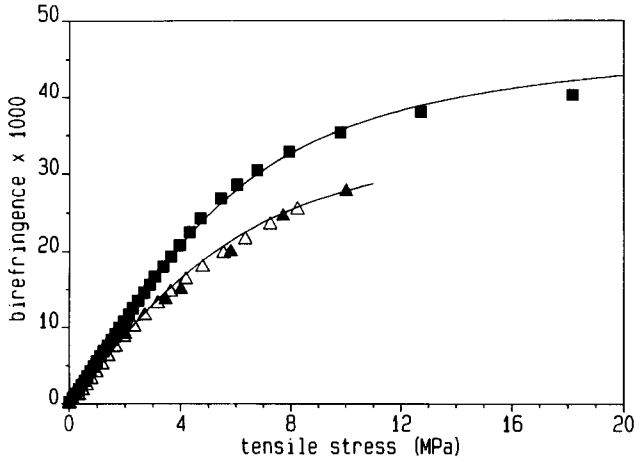

Figure 1 Equilibrium stress–optical behaviour of polystyrene (△, ▲) and polycarbonate (■). The values of temperature and strain rate are: (△) PS, $T = 120°C$, $\dot{\varepsilon} = 0.5\,s^{-1}$; (▲) PS, $T = 126°C$, $\dot{\varepsilon} = 0.1\,s^{-1}$ and; (■) PC, $T = 157°C$, $\dot{\varepsilon} = 0.025\,s^{-1}$

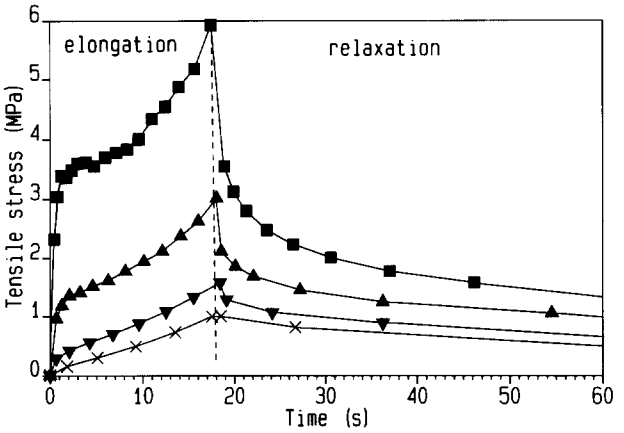

Figure 2 True tensile stress as a function of time for PS at various temperatures. The elongation at $\dot{\varepsilon} = 0.05\,s^{-1}$ is followed by stress relaxation at the same temperature: (×) 117; (▼) 111; (▲) 106 and; (■) 103°C

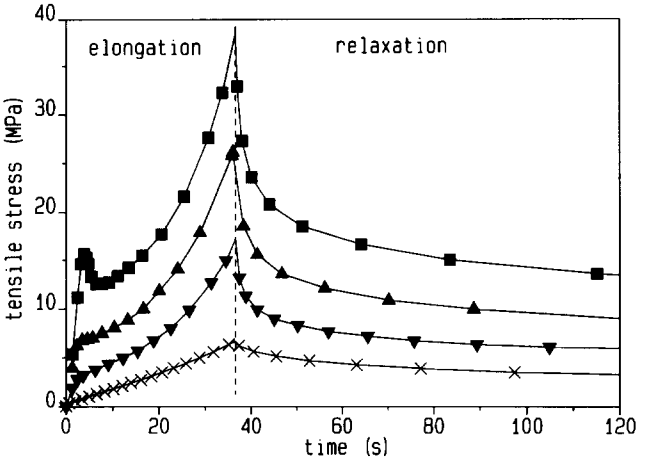

Figure 3 True tensile stress as function of time for PC at various temperatures. The elongation at $\dot{\varepsilon} = 0.025\,s^{-1}$ is followed by stress relaxation at the same temperature: (×) 155; (▼) 151; (▲) 147 and; (■) 142°C

In a second step, the stress–optical behaviour of the two polymers has been studied at temperatures closer to T_g, namely in the range 98.5–117°C for PS, and in the range 142–155°C for PC. The following mechanical test has been adopted: the specimens are stretched at constant elongational strain rate ($0.05\,s^{-1}$ for PS and $0.025\,s^{-1}$ for PC) up to a final extension ratio (L/L_0) of ~ 2.5 for all of the samples. The stress is then allowed to relax at constant deformation.

The curves in *Figures 2* and *3* show the time evolution of the true tensile stress during elongation and relaxation at various temperatures. It is observed that during elongation the stress rapidly reaches a threshold value and then increases more progressively. Similarly during the relaxation, σ first decreases rapidly by an amount close to its initial value during elongation, and then relaxes more slowly afterwards. The main effect of temperature on these curves is a pronounced increase of the initial threshold stress with decreasing temperature. For PC at 142°C, the true tensile stress even goes through a maximum during the first stage of elongation. The same stress overshoot is also found for PS at 98.5°C (see *Figure 9* below).

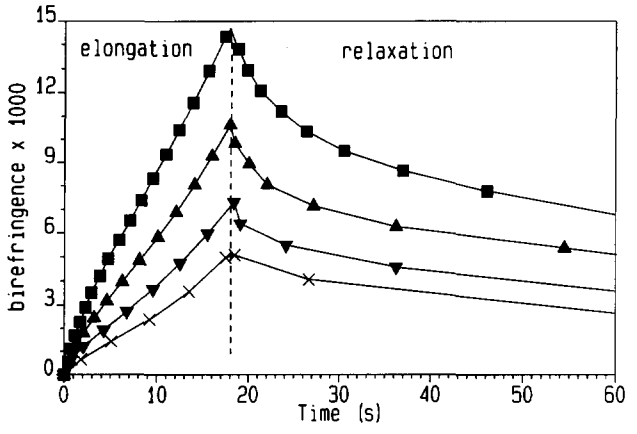

Figure 4 Birefringence as a function of time for PS samples at various temperatures. The elongation at $\dot{\varepsilon}=0.05\,s^{-1}$ is followed by stress relaxation at the same temperature: (×) 117; (▼) 111; (▲) 106 and; (■) 103°C

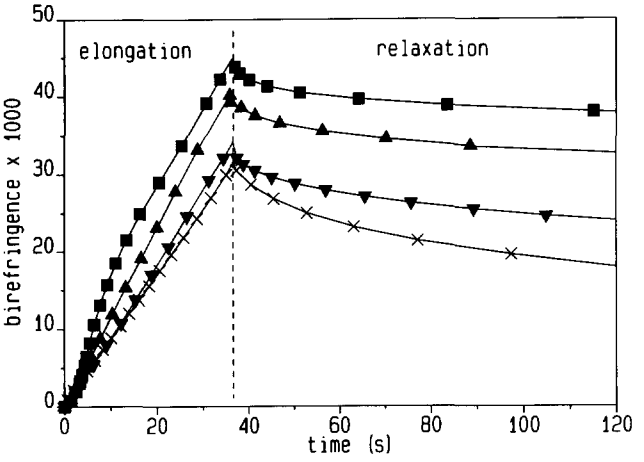

Figure 5 Birefringence as a function of time for PC samples at various temperatures. The elongation at $\dot{\varepsilon}=0.025\,s^{-1}$ is followed by stress relaxation at the same temperature: (×) 155; (▼) 151; (▲) 147 and; (■) 142°C

The birefringence for the same experiments has been plotted as a function of time in *Figures 4* and *5*. In contrast to the stress curves, the time evolution of birefringence shows no initial threshold value (and no overshoot): Δn increases and decreases smoothly during both elongation and relaxation.

If the above results for PS are plotted on a stress–optical diagram (i.e. birefringence *versus* stress), as in *Figure 1*, the curves in *Figure 6* are obtained. The data show that the equilibrium stress–optical law is obeyed for the elongation at 117°C and that there is only a slight deviation towards higher stress values at 111°C. For still lower temperatures, the deviation becomes more and more pronounced and indicates that the above discussed initial stress (~1 MPa at 106°C and 3 MPa at 103°C) does not apparently contribute to the birefringence. The stress and birefringence data at the lowest temperature, which have been plotted in *Figure 6* for the elongation as well as for the relaxation, clearly show a hysteresis. In stage (a) the stress first increases up to the initial value of 3 MPa, almost without any birefringence; this first step corresponds to a macroscopic deformation which is typically of the order of $\Delta L/L_0=10\%$. Stretching the specimen further (stage (b)) leads to an increase in both σ and Δn, but this occurs with stress values much higher than for the equilibrium behaviour. As soon as the elongation is stopped, the stress rapidly relaxes by an amount corresponding to its initial value during stretching, whereas the relaxation of birefringence is a much slower process over this same time-period (stage (c)). At the end of this third process, the representative point in the Δn–σ diagram is now on the equilibrium curve. In the final stage, (d), the relaxation of both stress and birefringence follows the equilibrium relationship.

To verify if the initial stress is really a material parameter (which is dependent on temperature and strain rate), the relationship between stress and birefringence has been characterized for a deformation history consisting of a first elongation at constant strain rate and a first stress relaxation, followed by a second elongation at the same strain rate and a second stress relaxation. As seen in *Figure 7*, the second elongation starts when the residual birefringence is of the order of 0.002, i.e. before complete relaxation of the chain orientation. The curve in *Figure 7* clearly shows that during the second elongation, the stress increases up to the initial value of the first elongation (~2 MPa) at almost constant birefringence, before both parameters increase together again. This result seems to indicate that the initial stress value appearing in the stress–optical curves during a stretching experiment does not depend on the level of orientation at a given temperature and strain rate.

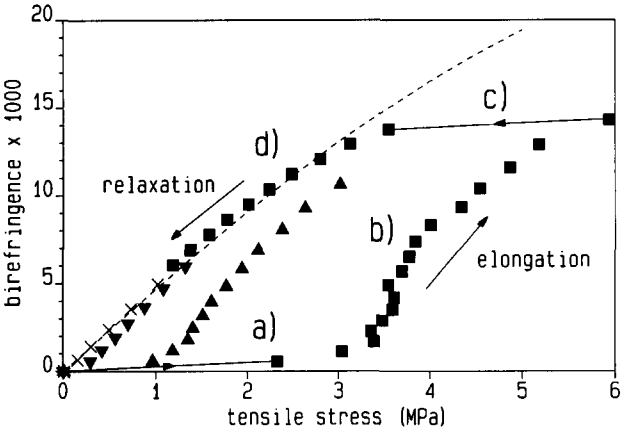

Figure 6 Birefringence as a function of stress for PS at various temperatures. The data are taken from *Figures 2* and *4*: (×) 117; (▼) 111; (▲) 106; (■) 103°C; the dotted line is the equilibrium curve of *Figure 1*. The elongation and relaxation at 103°C follow the cycle a–b–c–d (see text for details)

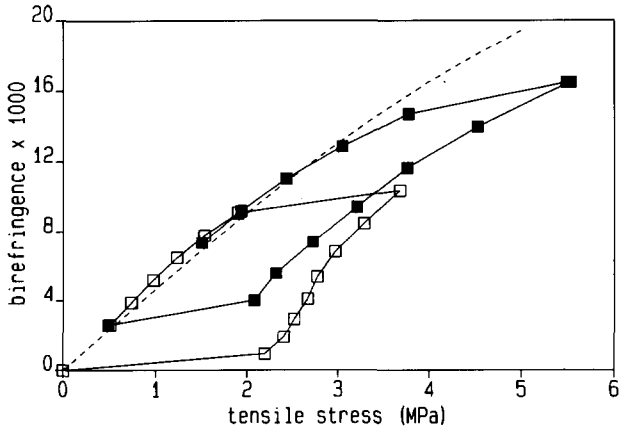

Figure 7 Birefringence as a function of tensile stress for PS at 99°C: (□) first elongation at $\dot{\varepsilon}=0.05\,s^{-1}$ up to a total extension ratio, $\lambda=2$ and stress relaxation during 300 s and; (■) second elongation, at the same strain rate, up to $\lambda=4$ and subsequent stress relaxation

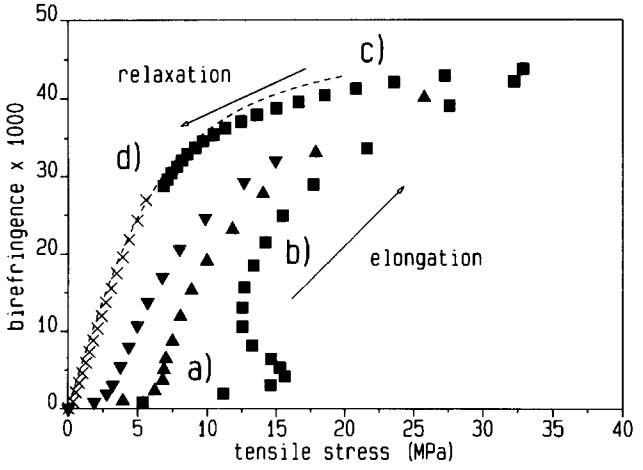

Figure 8 Birefringence as a function of stress for PC at various temperatures. The data are taken from *Figures 3* and *5*: (×) 155; (▼) 151; (▲) 147; (■) 142°C; the dotted line is the equilibrium curve of *Figure 1*. The elongation and relaxation at 142°C follow the cycle a–b–c–d (see text for details)

In *Figure 8* the stress–optical curves are plotted for PC at various temperatures. Here the equilibrium stress–optical behaviour during elongation is obeyed at 155°C whereas the same type of deviations as seen for PS are observed at lower temperatures. The hysteresis between σ and Δn during elongation and relaxation also exists for PC. Apart from the stress overshoot, the only difference between the data obtained at 103°C for PS and at 142°C for PC is that the initial relaxation process (step (c)), corresponding to the return to the equilibrium curve, is significantly slower for PC than for PS. This could be explained by the difference, T–T_g, which is smaller for PC than for PS.

The comparison between the time evolution of stress and birefringence during a constant strain rate stretching experiment suggests that the total tensile stress is made up of two contributions: (i) an entropic contribution arising from chain orientation and (ii) a second contribution related to the initial stress value, which is strongly temperature dependent and vanishes at temperatures higher than T_g+20°C. If we assume that the entropic contribution is related to the birefringence through the equilibrium stress–optical law, we can calculate its time evolution from that of the birefringence and the curves in *Figure 1*. This has been done for stretching experiments carried out at 98.5°C and 0.05 s^{-1} for PS, and at 142°C and 0.025 s^{-1} for PC.

In *Figures 9* and *10* the total stress and its entropic part, calculated from Δn, have been plotted as a function of the quantity $\lambda^2-\lambda^{-1}$, where λ is the extension ratio L/L_0. An almost linear behaviour is found for both PS and PC for the entropic part of the stress up to values of $\lambda \approx 2$. A neo-Hookean shear modulus can be calculated as the slope of these curves: values of approximately 1 and 3 MPa are found for PS and PC, respectively. Although these values are higher than the respective plateau moduli of the two polymers (i.e. 0.2 MPa for PS and 1 MPa for PC), their ratio is close to that of the plateau moduli value. Actually, the neo-Hookean moduli defined from the entropic part of the stress are closer to the values at the crossover between the $G'(\omega)$ and $G''(\omega)$ curves corresponding to the high frequency limit of the rubbery plateau (i.e. 0.5 MPa for PS and 2 MPa for PC).

The non-entropic contribution to the stress appears in *Figures 9* and *10* as the difference between the total and the entropic stress. It is found that the non-entropic stress remains almost constant during the stretching experiment, apart from the initial overshoot, which is observed only at temperatures very close to the T_g.

Flow-induced anisotropy in the solid state

After having discussed the stress–optical behaviour at temperatures close to the T_g, it is the aim of the second part of this paper to investigate the anisotropy of the solid-state properties as a function of the frozen-in orientation. In particular, we will try to characterize the influence of the two previously discussed contributions to the stress on the thermal expansion of PS samples in the direction of stretching. For this purpose, it will be necessary to freeze-in different levels of chain orientation by controlled cooling of the stretched specimens.

Freezing-in of the orientation. A series of PS specimens have been stretched at a given strain rate (0.05 s^{-1}) and temperature (102.2°C) up to the same extension ratio ($\lambda=2$). Once this stage is reached, three different ways of cooling to below the T_g have been used.

For the first specimen, the motors of the extensional rheometer are stopped and at the same time the sample

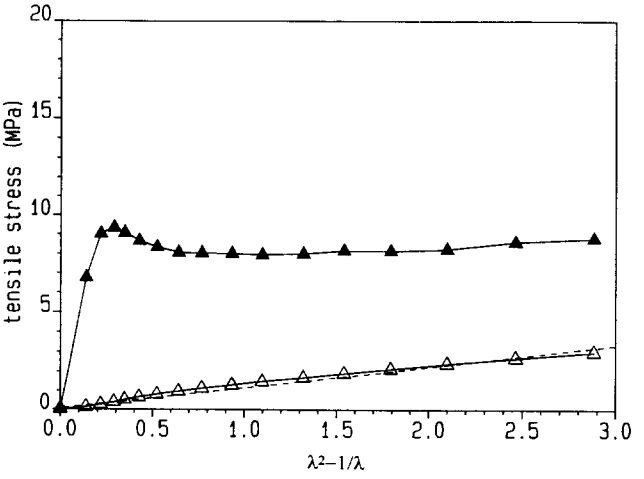

Figure 9 Total tensile stress (▲) and entropic stress (△), calculated from the birefringence, as a function of $\lambda^2-\lambda^{-1}$ for PS elongated at $\dot{\varepsilon}=0.05\ s^{-1}$ and $T=98.5$°C. Dotted line corresponds to a slope of 1 MPa

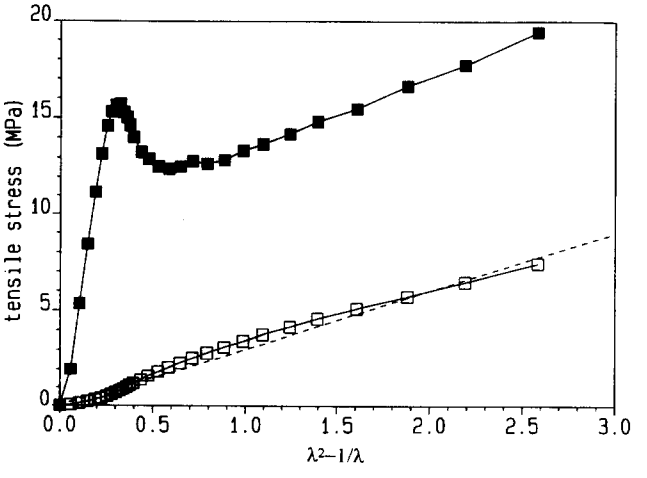

Figure 10 Total tensile stress (■) and entropic stress (□), calculated from the birefringence, as a function of $\lambda^2-\lambda^{-1}$ for PC elongated at $\dot{\varepsilon}=0.025\ s^{-1}$ and $T=142$°C. Dotted line corresponds to a slope of 3 MPa

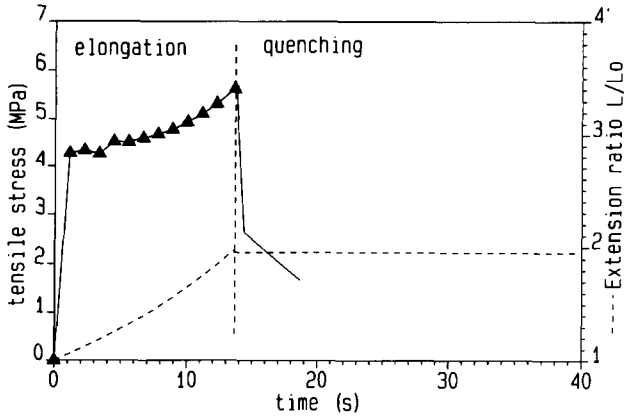

Figure 11 Stress (▲) and extension ratio (---) as a function of time during elongation at $\dot{\varepsilon}=0.05\,s^{-1}$ and quenching for sample 1

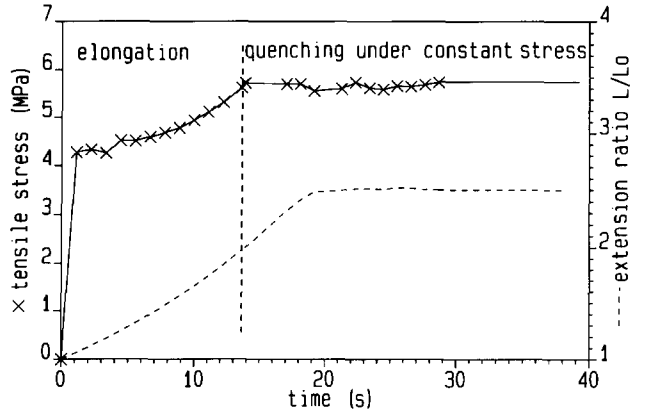

Figure 12 Stress (×) and extension ratio (---) as a function of time during elongation at $\dot{\varepsilon}=0.05\,s^{-1}$ and quenching for sample 2

is quenched by the removal of the oil bath; cooling thus occurs at a constant extension ratio (sample 1). Since it takes a few seconds for the temperature of the sample to decrease below the T_g, a significant part of the initial (non-entropic) stress has relaxed before the quenching is complete (see *Figure 11*).

To avoid this stress relaxation during quenching, in the case of the second specimen the servocontrol of the rheometer was switched over to a constant true tensile stress immediately after the constant strain rate stretching. At the same time, the oil bath is removed so that the whole cooling process down to room temperature occurs under constant-stress conditions (sample 2). *Figure 12* shows that after the constant strain rate stretching, the sample length further increases over a period of ~5 s, which corresponds to the cooling time below the T_g.

The birefringence values measured at room temperature are 0.0122 and 0.0178 for samples 1 and 2, respectively. *Figure 13* represents on a birefringence *versus* stress diagram the stretching and cooling stages of samples 1 and 2. From the curves in *Figure 6*, which showed that during relaxation the equilibrium stress–optical behaviour is recovered very rapidly, it can be assumed that this is also the case for sample 1. On the other hand, the measured birefringence for sample 2 is lower than its equilibrium value for the same stress, indicating that some part of the non-entropic stress contribution could be frozen-in for this sample.

It also seemed interesting to compare the anisotropy of the solid-state properties of sample 2 with those of a sample with the same birefringence but obeying the equilibrium stress–optical law. For this purpose, a third specimen (sample 3) has been stretched and quenched under the following conditions: after the standard stretching at a constant strain rate a constant true tensile stress is applied over a period of 20 s to the specimen at the same temperature. After that the motors of the extensional rheometer are stopped and the oil bath is removed as in the case of sample 1. During the isothermal creep, the length and the birefringence of the specimen both increase. Since the cooling occurs at a constant extension ratio, part of the stress relaxes at this time (see *Figure 14*) and it can be assumed that as with sample 1 the equilibrium stress–optical law is also satisfied for sample 3. With the particular choice of 20 s for the creep time, the final birefringence in sample 3 ($\Delta n \approx 0.0178$) is very close to that of sample 2.

Thermal expansion below the T_g. *Figure 15* shows the temperature dependence below the T_g of the relative length in the direction of stretching for samples 1, 2 and 3 together with that of an isotropic (unstretched) sample. Below 60°C, the observed behaviour is linear and a linear thermal expansion coefficient α can be determined for all samples. As expected, the value of $\alpha_{\parallel}$ in the direction of stretching for the oriented samples is lower than the expansion coefficient, α_0, of the isotropic sample.

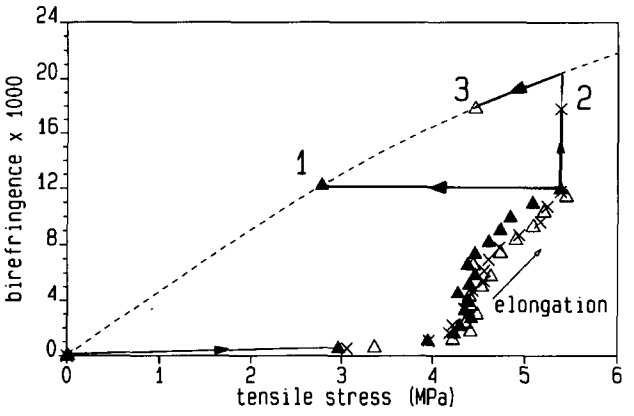

Figure 13 Birefringence as a function of stress during elongation and quenching of samples 1 (▲), 2 (×), and 3 (△). The curves obtained during the elongation stage give an idea of the reproducibility of the measurements

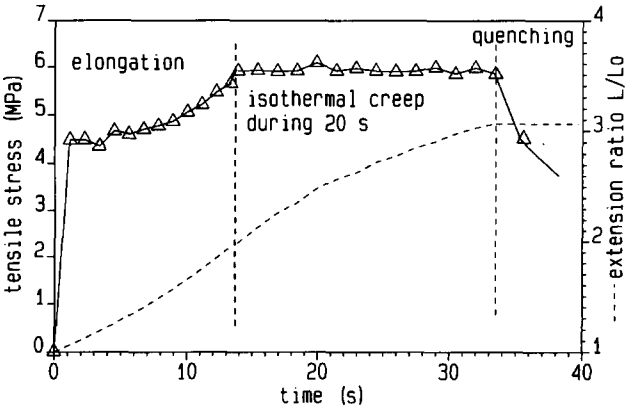

Figure 14 Stress (△) and extension ratio (---) as a function of time during elongation at $\dot{\varepsilon}=0.05\,s^{-1}$ and quenching for sample 3

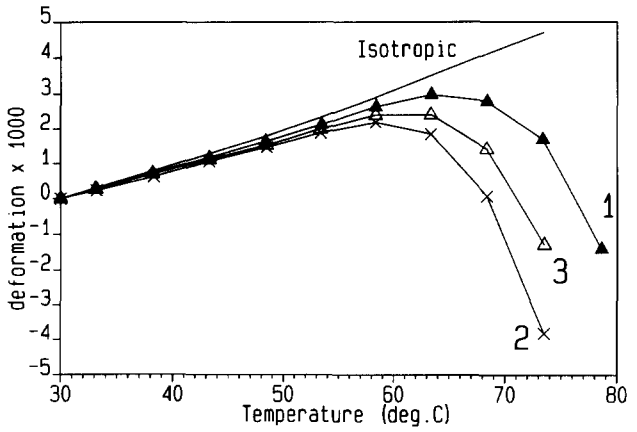

Figure 15 Temperature dependence of the relative variation of the sample length in the direction of stretching; $[L(T)-L(30°C)]/L(30°C)$, for the samples: 1 (▲); 2 (×); 3 (△); an isotropic (unstretched) sample is also shown for comparison purposes. The heating rate ($1° min^{-1}$) is low enough to provide temperature homogeneity within the sample

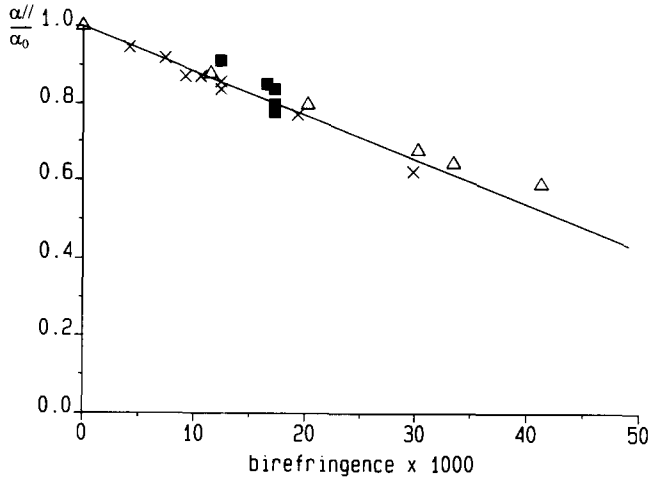

Figure 16 Relative thermal expansion coefficient $\alpha_{\parallel}/\alpha_0$ in the direction of stretching as a function of birefringence: (×) data taken from ref. 11; (△) data taken from ref. 12 and; (■) results obtained in this study

Figure 16 shows the ratio $\alpha_{\parallel}/\alpha_0$ as a function of the birefringence according to our experimental results, together with data on PS from the literature[11,12]; to within experimental error, it can be seen that the agreement is satisfactory. Nevertheless, the effect of orientation on the thermal expansion coefficient remains small for values of birefringence lower than 0.02 and it is difficult for example to discriminate, from *Figure 15*, between the behaviour of samples 2 and 3. Actually, the major effect, which arises at temperatures of about 60°C and appears as a negative thermal expansion, is an elastic recovery of the elongated samples. The recoverable deformations reported in *Figure 15* are not equilibrium values and depend in fact on the heating rate; if the temperature is kept constant, the recovery increases with time. Whereas little difference between samples 1, 2 and 3 is found for the linear thermal expansion coefficient below 60°C, the recovery at higher temperatures depends clearly on the way the samples have been quenched. There is in particular a marked difference between samples 2 and 3, which have the same birefringence: the recovery is the strongest (and also starts at the lowest temperature) for sample 3, which has been cooled under constant stress conditions.

CONCLUSIONS

The results of the present study confirm that the linear stress–optical law for PS and PC in simple extension is only verified at low stresses and high temperatures (typically above $T_g + 20°C$). Deviations from the (high temperature) equilibrium behaviour appearing at temperatures close to the T_g can be qualitatively explained by considering the tensile stress as the sum of two contributions, namely an entropic stress related to the birefringence through the equilibrium stress–optical law and a non-entropic part which remains almost constant during extension at a constant strain rate.

On the other hand, our data show that significant recoverable strains can appear below the T_g in specimens that have been stretched at high stress levels in the melt and then rapidly quenched. The order of magnitude of the recoverable deformations that are involved (0.5–1%) are far from being negligible with respect, for example, to the warping of injection moulded parts. Moreover, our data show that the temperatures at which this recovery occurs can be as low as T_g–35°C, depending on the frozen-in orientation. Finally, the potential recoverable strain below the T_g is not solely a function of the orientational birefringence, as has been confirmed by the different behaviour of samples 2 and 3, but also appears to depend on the non-entropic contribution to the stress.

Since the stresses arising in injection moulding are comparable to those used in the present study, an accurate simulation of the final shape and dimensions of injection moulded parts will need a model for the thermoviscoelastic transition, both below and above T_g, in order to be able to describe the type of elastic recovery shown in *Figure 15*.

ACKNOWLEDGEMENTS

We thank the French Ministère de la Recherche, the 'Club des Logiciels de l'Industrie Plastique' and the PSA Company for financial and technical support.

REFERENCES

1 Struik, L. C. E. 'Internal Stresses, Dimentional Instabilities and Molecular Orientation in Plastics', Wiley, Chichester, 1990, Ch. 4, p. 293
2 Janeschitz-Kriegl, H. 'Polymer Melt Rheology and Flow Birefringence', Springer, Berlin, 1983
3 Choy, C. L. in 'Developments in Oriented Polymers-1' (Ed. I. M. Ward), Applied Science, London, 1982, p. 121
4 Retting, W. *Colloid Polym. Sci.* 1979, **257**, 689
5 Inoue, T., Okamoto, H. and Osaki, K. *Macromolecules* 1991, **24**, 5670
6 Read, B. E. *Polym. Eng. Sci.* 1983, **23**, 835
7 Muller, R. and Froelich, D. *Polymer* 1985, **26**, 1477
8 Matsumoto, T. and Bogue, D. C. *J. Polym. Sci., Polym. Phys. Edn* 1977, **15**, 1663
9 Wimberger-Friedl, R. and De Bruin, J. G. *Rheol. Acta* 1991, **30**, 419
10 Treloar, L. R. G. 'The Physics of Rubber Elasticity', Clarendon Press, Oxford, 1949, p. 144
11 Retting, W. *Colloid Polym. Sci.* 1981, **259**, 52
12 Wang, L. H., Choy, C. L. and Porter, R. S. *J. Polym. Sci., Polym. Phys. Edn* 1982, **20**, 633